J. Membrane Biol. 146, 211–224 (1995)

The Journal of
Membrane
Biology

Lumenal Calcium Modulates Unitary Conductance and Gating of a Plant Vacuolar Calcium Release Channel

E. Johannes, D. Sanders
The Plant Laboratory, Biology Department, University of York, PO Box 373, York Y01 5YW, UK

Received: 28 November 1994/Revised: 16 March 1995

Abstract. The patch clamp technique has been used to investigate ion permeation and Ca^{2+}-dependent gating of a voltage-sensitive Ca^{2+} release channel in the vacuolar membrane of sugar beet tap roots. Reversal potential measurements in bi-ionic conditions revealed a sequence for permeability ratios of $Ca^{2+} \approx Sr^{2+} \approx Ba^{2+} > Mg^{2+} \gg K^+$ which is inversely related to the size of the unitary conductances $K^+ \gg Mg^{2+} \approx Ba^{2+} > Sr^{2+} \approx Ca^{2+}$, suggesting that ion movement is not independent. In the presence of Ca^{2+}, the unitary K^+ current is reduced in a concentration- and voltage-dependent manner by Ca^{2+} binding at a high affinity site ($K_{0.5}$ = 0.29 mM at 0 mV) which is located 9% along the electric field of the membrane from the vacuolar side. Comparison of reversal potentials obtained under strictly bi-ionic conditions with those obtained in the presence of mixtures of the two ions indicates that the channel forms a multi-ion pore. Lumenal Ca^{2+} also has an effect on voltage-dependent channel gating. Stepwise increases of vacuolar Ca^{2+} from micromolar to millimolar concentrations resulted in a dramatic increase in channel openings over the physiological voltage range via a shift in threshold for channel activation to less negative membrane potentials. The steepness of the concentration dependence of channel activation by Ca^{2+} at –41 mV predicts that two Ca^{2+} ions need to bind to open the gate. The implications of the results for ion permeation and channel gating are discussed.

Key words: Calcium-permeable channel — Permeation — Selectivity — Gating — Calcium modulation — *Beta vulgaris*

Correspondence to: E. Johannes

Introduction

Ca^{2+}-permeable channels in the plasma and vacuolar membranes of plant cells play a crucial role in stimulus-evoked elevation of cytosolic free Ca^{2+} concentration which is known to trigger a wide array of physiological responses (Johannes, Brosnan & Sanders, 1991; Schroeder & Thuleau, 1991; Bush, 1993). Opening of these channels leads to dissipative Ca^{2+} fluxes into the cytoplasm along the steep electrochemical potential gradient for Ca^{2+} which exists across the plasma membrane and vacuolar membrane. Voltage-gated and stretch-activated Ca^{2+}-permeable channels have been identified in the plasma membrane (Cosgrove & Hedrich, 1991; Ding & Pickard, 1993, Thuleau et al., 1994; Piñeros & Tester, 1995) and a large variety of Ca^{2+}-permeable channels have been detected in the vacuolar membrane (*see* references below) which surrounds the principal Ca^{2+} store in mature cells.

Ca^{2+} can be mobilized from the vacuole both through ligand-operated channels which open in the presence of inositol 1,4,5-trisphosphate (e.g., Alexandre, Lassalles & Kado, 1990; Brosnan & Sanders, 1990; Allen & Sanders, 1994*b*) and through voltage-operated channels (e.g., Johannes, Brosnan & Sanders, 1992*a,b;* Johannes, Allen & Sanders 1994; Gelli & Blumwald, 1993; Allen & Sanders, 1994*a*) which are gated open when the vacuolar membrane potential is shifted cytosol-negative over the physiological range. The transtonoplast membrane potential is normally kept negative (–10 to –50 mV) through the action of electrogenic H^+ pumps which transport H^+ into the vacuolar lumen (Rea & Sanders, 1987). Ca^{2+}-permeable channels which open at positive vacuolar membrane potentials have also been described (Pantoja, Gelli & Blumwald, 1992; Ping, Yabe & Muto, 1992*a,b;* Ward & Schroeder, 1994). Although many of the basic features of these channels have now

been characterized at the single channel level, a detailed analysis of ion permeation and channel gating is missing.

Electrophysiological studies on L-type Ca^{2+} channels in animal cells have revealed that their high Ca^{2+} selectivity is achieved by high affinity binding sites in the channel pore (Tsien et al., 1987). The Ca^{2+} affinity of these binding sites and their location in the electric field of the membrane were mapped using the Woodhull (1973) model of voltage-dependent block of the unitary monovalent ionic current by Ca^{2+} (Rosenberg & Chen, 1991).

In the present study, we have adopted a similar approach to determine the properties of Ca^{2+} binding sites involved in selectivity and ion permeation through a voltage-gated Ca^{2+}-permeable channel in the vacuolar membrane of sugar beet tap roots. Some of the fundamental attributes of the channel have been described by us previously (Johannes et al., 1992*a,b*). The channel has a 15-fold higher permeability for Ca^{2+} over K^+ when tested in bi-ionic conditions and shows saturation of the unitary Ca^{2+} current at large negative potentials. Voltage-activation is instantaneous and the open state probability increases dramatically over the negative voltage range. Channel activity is further enhanced when lumenal Ca^{2+} is increased. While Ca^{2+} is required on the lumenal side to activate the channel, variation of cytoplasmic Ca^{2+} has no significant effect on the Ca^{2+} release current. The channel is insensitive to inositol 1,4,5-trisphosphate but blocked by Gd^{3+} and Zn^{2+}.

In this report, we provide a more thorough analysis of ion permeation and selectivity and also a detailed investigation of the voltage- and Ca^{2+}-dependent gating in order to characterize Ca^{2+} binding to the gate. Tests with other divalent cations were carried out to elucidate the specificity of the response. The results are compared with similar studies on other channels in plant and animal cells where appropriate, and the physiological implications are discussed.

Materials and Methods

Isolation of Vacuoles and Composition of Patch Clamp Media

Vacuoles were isolated from fresh sugar beet tap roots grown in the field or greenhouse. The tissue was sliced with a sharp razor blade and the vacuoles were rinsed from the cut surface directly into the recording chamber (Hedrich & Neher, 1987) with Medium I (*see below*) supplemented with 1 mM $MgCl_2$. The osmolarity of the patch clamp media (measured by freezing point depression with a Camlab Model 200 osmometer) was adjusted with sorbitol to a value 10% higher than that of the cell sap. In lumenal-side out patches the pipette solution (Medium I) comprised (in mM): 40 KOH, 10 KCl, 0.5 DL-dithiothreitol (DTT), adjusted with 10 N-[2-hydroxyethyl]piperazine-N′-[2-ethanesulfonic acid] (HEPES) and 20 dimethylglutaric acid to pH 7.3. The Ca^{2+} concentration of Medium I was $<10^{-8}$ M, as determined with Ca^{2+}-selective microelectrodes. For cytoplasmic-side out patches, the pipette solution contained Medium I plus 0.3 mM $CaCl_2$. Deviations from this composition and details of bath solutions are given in the figure legends. In some experiments, dimethylglutaric acid was replaced by gluconic acid. This did not cause any significant change in the single channel current or gating behavior. We found, however, that a high Cl^- concentration in the solutions (>20 mM) caused activation of other channels (*see also* Plant, Gelli & Blumwald, 1994). During the recording the preparation was constantly perfused with two peristaltic pumps (Gilson Minipuls 3) which allowed exchange of test media. Isolated vacuoles were washed for at least 15 min in Medium I plus 1 mM $MgCl_2$ before forming a seal. Experiments were performed at room temperature (25°C).

Patch Clamp Procedure and Data Acquisition

Patch clamp experiments were carried out as described by Hamill et al. (1981). The reference Ag/AgCl half-cell was filled with Medium I (without DTT) and connected to the bath via an agar bridge (3% agar in Medium I). Clamp voltages were controlled with an EPC-7 patch clamp amplifier (List Electronics, Darmstadt, Germany). Data were recorded on digital audiotape (DTC-1000 ES; Sony Corporation, Tokyo, Japan). For further analysis with the CED (Cambridge Electronic Design, Cambridge, UK) software package the data were low pass filtered (8-pole Bessel filter) at 300 Hz or 500 Hz and digitized at 1.5 kHz and 2.5 kHz (1401 A/D converter, Cambridge Electronic Design), respectively.

Pipettes were pulled from borosilicate glass capillaries (Kimax, thinwalled) and coated with Sylgaard. Typical resistances of pipettes used for lumenal-side-out recordings were 20 MΩ in Medium I. Lower resistance pipettes (8 MΩ) were used for cytoplasmic-side-out patches which were obtained after the establishment of a vacuole-attached seal by breaking the membrane with bipolar pulses (±0.8 V, 5–10 msec each) and drawing the pipette away from the vacuole.

Sign Convention and Liquid Junction Potentials

Vacuolar membrane potentials and currents are presented according to the convention for measurements on endomembranes (Bertl et al., 1992) which uses the vacuolar lumen as a reference. Thus inward currents are those that flow into the cytosol. This convention is also adopted when we refer to other studies, regardless of which convention the authors use in the original report.

Liquid junction potentials were calculated according to Barry & Lynch (1991) or measured as described by Neher (1992) and subtracted from the pipette potential in vacuolar-side out patches. Liquid junction potentials were highest (around 13 mV) when bi-ionic conditions were used.

Data Analysis and Presentation

Permeability ratios for mixtures of divalent and monovalent cations were determined with Eq. 1 which was obtained after transformation of the Goldman-Hodgkin-Katz current equation (*see* Hille, 1992):

$$\frac{P_{Ca^{2+}}}{P_{K^+}} = -\frac{(a_{K^+_{cyt}} - a_{K^+_{vac}} e^{-(EF/RT)})\,(1 - e^{-2(EF/RT)})}{4(a_{Ca^{2+}_{cyt}} - a_{Ca^{2+}_{vac}} e^{-2(EF/RT)})\,(1 - e^{-(EF/RT)})}, \quad (1)$$

where E is the reversal potential, $a_{x_{cyt,vac}}$ are the activities of ion X in the cytoplasmic and vacuolar compartments, respectively, and R, T and F have their usual meanings. Ion concentrations were multiplied by their

activity coefficients which were estimated according to the Debye & Hückel equation (Eq. 2; in Skoog & West, 1982):

$$-\log\gamma = \frac{0.5085z^2\sqrt{\mu}}{1+0.3281A\sqrt{\mu}}, \quad (2)$$

where γ is the activity coefficient, z is the charge of the ion, μ is the ionic strength of the solution and A is the effective diameter of the hydrated ion in Ångström units.

For determination of the open state probability of the channel, the ratio of the mean open time to the total recording time was derived from amplitude histograms as described by Bertl & Slayman (1990). This value was divided by the maximum number of simultaneously open channels. Recordings of 30 sec duration which did not display activity by other channel types were used for the analysis.

Single channel current voltage curves were constructed from measurements of similar quality as those displayed in Fig. 5 and Fig. 4*A*. The absence of significantly more noise in the open state compared with the closed state of the channel suggests that the open channel current is not attenuated by rapid openings and closings. The unitary slope conductance for divalent cations was calculated from the linear section (fitted by eye) of the current voltage curve negative of the reversal potential.

For clarity, the figures show representative measurements (obtained on a single patch) from data sets of three to ten independent recordings. While unitary current measurements were highly reproducible (standard deviations <8%), the open state probabilities were more variable because of uncertainty about the true number of channels in the patch.

Results

Selectivity for Divalent Cations

The selectivity for divalent cations of the voltage-gated Ca^{2+}-permeable channel in the vacuolar membrane of sugar beet tap roots was tested in lumenal-side-out patches under bi-ionic conditions. With 50 mM K^+ on the cytoplasmic side and 10 mM Ca^{2+} on the lumenal side, the single channel K^+ outward current increases with voltage to yield a conductance of 200 pS at more positive potentials where linearity is approached (Fig. 1, inset). The inward Ca^{2+} current, however, increases with a slope conductance of 11 pS and saturates with negative-going voltage to a maximum level of about 0.5 pA. The slope conductance and saturation current are independent of the vacuolar Ca^{2+} concentration in the range of 5 to 40 mM (Johannes et al., 1992*a*). The unitary current reverses at 22–26 mV from which a permeability ratio for Ca^{2+} over K^+ of 14–18:1 can be determined using Eq. 1. Substitution of vacuolar Ca^{2+} with equimolar concentrations of Mg^{2+}, Sr^{2+} and Ba^{2+} (all tested at 10 mM) revealed that Mg^{2+} has a lower relative permeability than Ca^{2+} ($P_{Mg^{2+}}:P_{K^+} \approx 9:1$) whereas the reversal potentials in the presence of Ba^{2+} and Sr^{2+} are similar to that obtained with Ca^{2+} (Fig. 1., Table). All divalent cations show strong saturation of the unitary current when the voltage is shifted negative, with Mg^{2+} and Ba^{2+} carrying larger currents than Ca^{2+} and Sr^{2+} (Table, Fig. 1.). From a range of other divalent cations tested (Zn^{2+}, Ni^{2+}, Co^{2+}, Mn^{2+}), only Mn^{2+} was able to permeate the channel (*data not shown*). Although the unitary current carried by 10 mM Mn^{2+} was similar to that obtained with Mg^{2+} and Ba^{2+}, channel activity in the presence of Mn^{2+} was reduced to occasional short openings (*cf.* Fig. 8.).

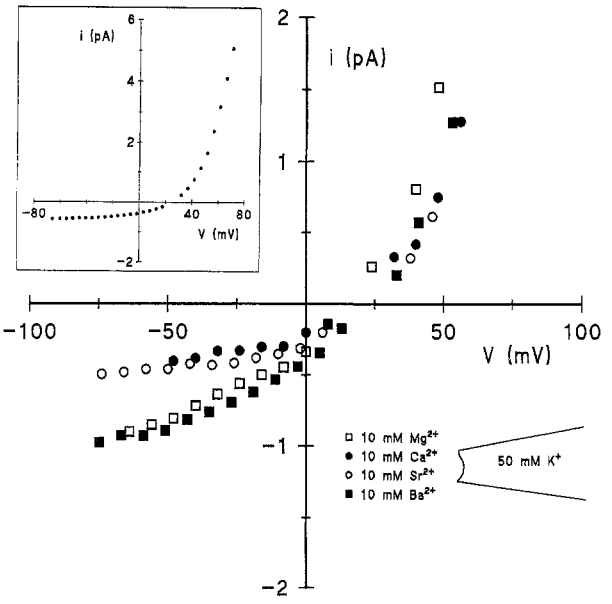

Fig. 1. Single channel current-voltage characteristics in bi-ionic conditions. Lumenal-side-out patch with (in mM): 20 KCl, 30 K gluconate in the pipette and 10 $MgCl_2$ (□), 10 $CaCl_2$ (●), 10 $SrCl_2$ (○), 10 $BaCl_2$ (■), respectively, in the bath. pH was adjusted to pH 7.3 with 2 mM Tris + HEPES. Liquid junction potentials were ≈13 mV. Details of conductances, saturation currents and reversal potentials are given in the Table. Inset: Extended current voltage curve with 10 mM $CaCl_2$ in the bath. The K^+ outward current has a conductance of 200 pS.

Table. Unitary slope conductance, saturation current carried by various divalent cations, and respective reversal potentials

	Unitary conductance (pS)	Reversal potential (mV)	Saturation current (pA)	$P_{x^{2+}} : P_{K^+}$
Mg^{2+}	17.4 ± 1.2	15.4 ± 1.6	−1.13 ± 0.11	8.8
Ca^{2+}	11.7 ± 1.2	21.8 ± 0.8	−0.47 ± 0.03	14.1
Sr^{2+}	10.9 ± 0.6	22.5 ± 1.7	−0.48 ± 0.02	15.2
Ba^{2+}	17.0 ± 1.5	22.2 ± 1.5	−1.20 ± 0.21	14.9

Derived from measurements in bi-ionic conditions as shown in Fig. 1 (data set of five independent recordings). Details of the ionic composition of the media are given in the legend of Fig. 1. The permeability ratios were calculated with Eq. 1 using activity coefficients derived from Eq. 2 (*see* Materials and Methods).

Ca^{2+} Binding Sites Assure Ca^{2+} Selectivity

While the permeability ratio determined from the reversal potential in bi-ionic conditions indicates that Ca^{2+} is

the favored ion, the absolute permeability represented by the unitary current is much higher for K^+. This apparent discrepancy shows that Ca^{2+} and K^+ do not move through the channel independently but compete for binding sites in the channel pore. A similar observation has been made in L-type Ca^{2+} channels in animal cells where at least two Ca^{2+} binding sites represented by four conserved glutamate residues in the pore lining regions of the α_1 subunit of the channel protein have been detected (Rosenberg & Chen, 1991; Yang et al., 1993).

To obtain further information on the affinity and location of the putative Ca^{2+} binding site(s) in the voltage-sensitive Ca^{2+}-permeable channel in sugar beet, the effects of lumenal Ca^{2+} on the K^+ inward current were tested. Increasing concentrations of Ca^{2+} were added to the bathing medium of lumenal-side-out patches originally held in symmetrical 50 mM K^+. The current voltage relationships (Fig. 2*A*.) reveal a dose- and voltage-dependent decrease in the inward current when lumenal Ca^{2+} is elevated. In the presence of low lumenal Ca^{2+} concentrations (0.03–1 mM), the inward current is predominantly carried by K^+. The effect of Ca^{2+} on this current was assessed with the Woodhull (1973) model of voltage-dependent ion block to obtain information on the affinity and location of the binding site. The percentage inhibition of the inward current as a function of vacuolar Ca^{2+} follows Michaelis-Menten kinetics (Fig. 2*B*.). Since channel activity strictly depends on the presence of divalent cations on the vacuolar side (Johannes et al., 1992*b*), the control inward current in the absence of Ca^{2+} was extrapolated from the outward current (dotted line in Fig. 2A.) assuming that the channel is symmetrical with respect to K^+ permeation. The Ca^{2+} concentration where inhibition of the K^+ current is half maximal ($K_{0.5}$) was determined for a range of negative voltages and the voltage-dependence of the binding constants is depicted in Fig. 2*C*. in a semi-logarithmic plot. The affinity constant for Ca^{2+} binding decreases (i.e., the affinity for Ca^{2+} increases) when the cytoplasmic side becomes increasingly negative with respect to the vacuolar lumen and follows Eq. 3 (Woodhull 1973):

$$K_{0.5} = K_{0.5}^{V=0}\, e^{\delta 2FV/RT}, \qquad (3)$$

where $K_{0.5}^{V=0}$ is the binding constant at $V = 0$ mV and δ is the fractional electrical distance from the bulk solution to the binding site. *R, T, F* have their usual meanings. From the steepness of the voltage-dependence a fractional electrical distance of 0.09 can be calculated; and the extrapolated $K_{0.5}^{V=0}$ value for Ca^{2+} binding at $V = 0$mV is 0.29 mM (Fig. 2*C*.). This suggests that the binding site is located approximately 9% through the electrical field into the pore from the vacuolar side and that its affinity for Ca^{2+} is moderate compared with L-type Ca^{2+} channels in animal cells which have $K_{0.5}$ values in the micromolar range (Tsien et al., 1987).

To probe for Ca^{2+} binding sites near the cytoplasmic face of the channel, reciprocal measurements were carried out in which Ca^{2+} on the cytoplasmic side was varied in cytoplasmic-side-out patches. However, when cytoplasmic Ca^{2+} was elevated above contaminating levels of approximately 10 nM (lowest concentration tested: 0.03 mM), the outward current was blocked and no open channel current could be determined after step pulsing the voltage from a negative value where channel activity is high to the positive range. Although this prevents characterization of binding sites towards the cytoplasmic side of the membrane, there are indications that the channel can hold more than one ion at the same time. Thus, the current-voltage relationships shown in Fig. 3. demonstrate that the reversal potentials are about 5:1 in favor of Ca^{2+} when mixtures of Ca^{2+} and K^+ are used as charge carriers at the vacuolar side compared with permeability ratios of 17:1 obtained under bi-ionic conditions (Fig. 3., inset). These observations suggest that the channel is a multi-ion pore (Hille, 1992). Furthermore, the current-voltage characteristics show that the saturation current obtained in the mixture of 50 mM K^+ and 25 mM Ca^{2+} is higher than that with Ca^{2+} alone (Fig. 3.). This means that the K^+ inward current is not completely blocked by 25 mM Ca^{2+} which could indicate the presence of a second binding site with a lower affinity for Ca^{2+}.

Effects of Lumenal Ca^{2+} on Channel Gating

In a previous study, we reported that elevation of vacuolar Ca^{2+} in the range of 5–20 mM enhanced channel activity over the physiological voltage range between −10 and −50 mV (Johannes et al., 1992*a*). However as

Fig. 2. Dose- and voltage-dependent inhibition of the unitary K^+ current by lumenal Ca^{2+}. (*A*) Single channel current voltage characteristics showing the effect of lumenal Ca^{2+} on the unitary K^+ inward current. Representative measurements from ten independent recordings. Lumenal-side-out patch in symmetrical Medium I with 0.03 mM $CaCl_2$ (●), 0.1 mM $CaCl_2$ (○), 0.3 mM $CaCl_2$ (▲), and 1 mM $CaCl_2$ (△) added to the bath. The dotted line shows the theoretical K^+ inward current in the absence of Ca^{2+} and is extrapolated from the K^+ outward current. (*B*) Inhibition of the unitary inward current by vacuolar Ca^{2+} ($[Ca^{2+}]_{vac}$) at V = −40 mV and V = −80 mV, respectively. The data are taken from (*A*) and fitted to the Michaelis-Menten equation with a nonlinear least-squares method from which $K_{0.5}$ values of 0.22 mM (V = −40 mV) and 0.16 mM (V = −80 mV) were determined. (*C*) Semi-logarithmic plot of the $K_{0.5}$ values as a function of the vacuolar membrane potential. The data were fitted by nonlinear least-squares to Eq. 3, from which an electrical distance from the bulk solution to the Ca^{2+} binding site of $\delta = 0.089 \pm 0.03$ and a value for $K_{0.5}^{V=0}$ of 0.292 ± 0.003 mM were derived.

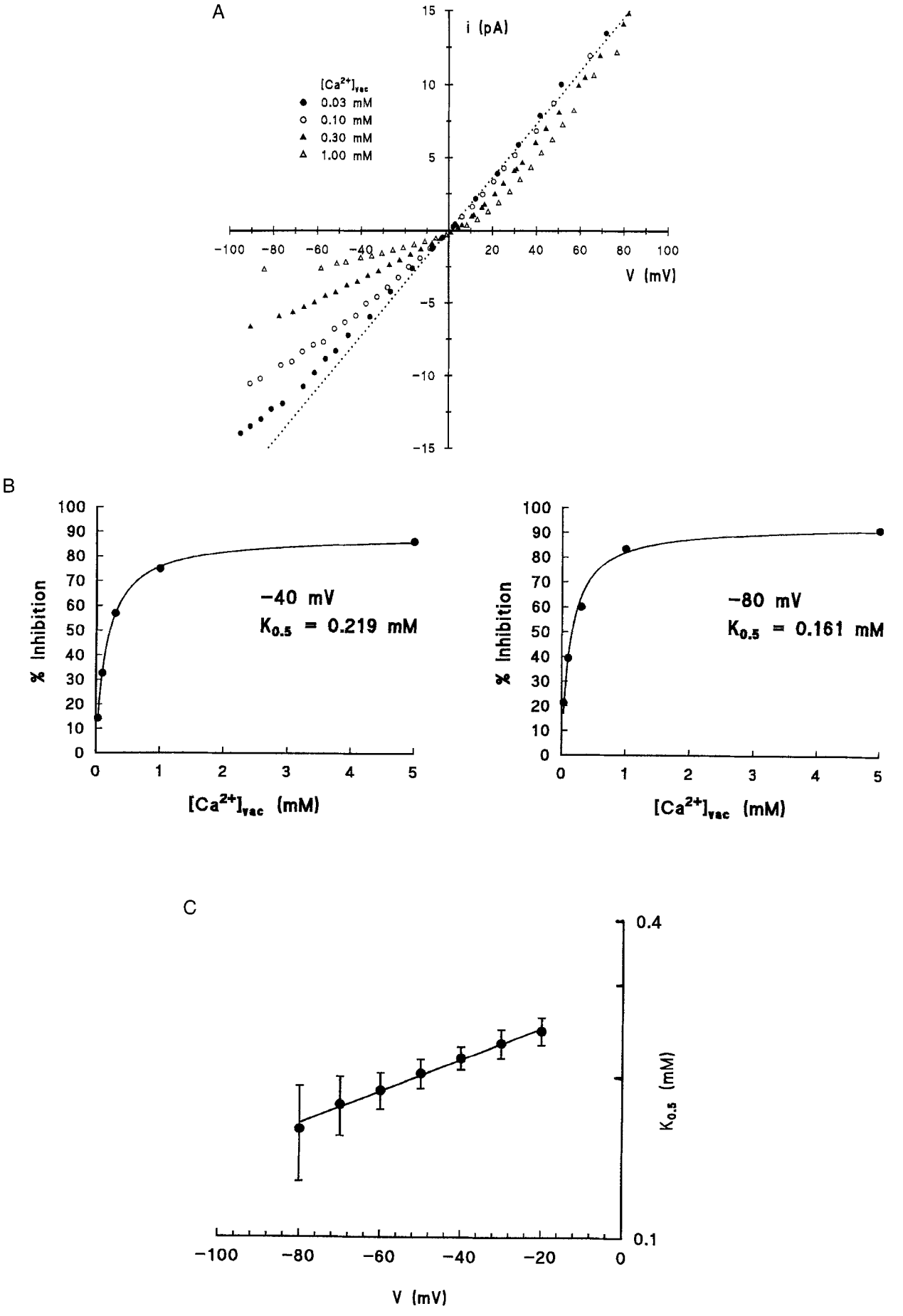
A
i (pA)
$[Ca^{2+}]_{vac}$
0.03 mM
0.10 mM
0.30 mM
1.00 mM
V (mV)
B
% Inhibition
−40 mV
$K_{0.5}$ = 0.219 mM
$[Ca^{2+}]_{vac}$ (mM)
% Inhibition
−80 mV
$K_{0.5}$ = 0.161 mM
$[Ca^{2+}]_{vac}$ (mM)
C
$K_{0.5}$ (mM)
V (mV)

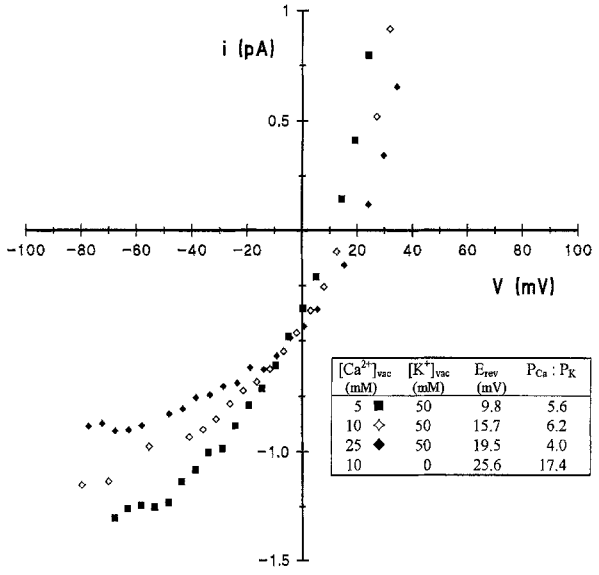

Fig. 3. Current voltage characteristics of a lumenal-side-out patch successively bathed in (mM): 40 KOH, 10 KCl, 5 $Ca(OH)_2$, 10 HEPES, 25.2 dimethylglutaric acid (■), 40 KOH, 10 KCl, 10 $Ca(OH)_2$, 10 HEPES, 37 dimethylglutaric acid (◇) and 40 KOH, 10 KCl, 25 $Ca(OH)_2$, 10 HEPES, 45.2 dimethylglutaric acid (♦). pH of the bath solutions was 7.3 and Medium I was used in the pipette. Liquid junction potentials were 0.9 mV and 2.2 mV in conditions with 10 mM Ca^{2+} and 25 mM Ca^{2+}, respectively. Inset: Reversal potentials (E_{rev}) and permeability ratios ($P_{Ca^{2+}}$:P_{K^+}) calculated with Eqs. (1) and (2) for the conditions shown above and also for measurement with 10 mM $Ca(OH)_2$, 10 mM HEPES, 8.4 mM dimethylglutaric acid pH 7.3 in the bath (current-voltage relationship not shown for clarity but *cf.* Fig. 1.). Average values of five independent measurements, with all four solutions tested on the same patch.

discussed below, changes in the ionic strength of the solution also affect channel gating. Figure 4. shows that addition of the impermeant cation N-methylglucamine (NMG) increases the open frequency of the channel while simultaneously decreasing the unitary conductance. Since no concomitant shift in the reversal potentials is observed, it is likely that NMG compensates surface charges at the channel entrance (Green & Andersen, 1991). Therefore the effect of lumenal Ca^{2+} was reinvestigated in conditions where the ionic strength is kept fairly constant, i.e., in a background of 50 mM K^+ and with lower vacuolar Ca^{2+} concentrations. This also represents a more physiological condition since lumenal Ca^{2+} is in the lower millimolar range (Felle, 1988) and K^+ between 30 and 200 mM (Leigh & Wyn-Jones, 1984; Maathuis & Sanders, 1993).

As reported previously the channel is completely inactive in the absence of divalent cations on the vacuolar side (Johannes et al., 1992*b*). Upon addition of increasing amounts of vacuolar Ca^{2+}, a concentration-dependent increase in channel opening frequency is observed. This is demonstrated in Fig. 5. which shows single channel current traces obtained with a lumenal-side-out patch clamped at −24 mV with increasing

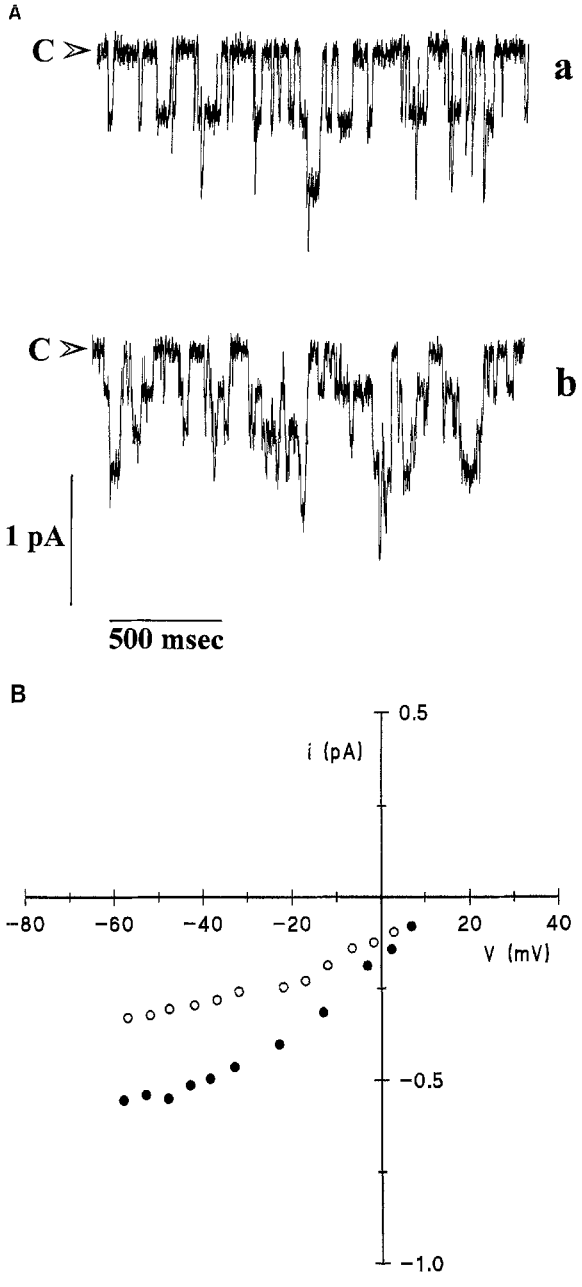

Fig. 4. Effect of N-methylglucamine on unitary Ca^{2+} current and channel activity. (*A*) Single channel current traces from a lumenal-side-out patch held at V = −54 mV. (*a*) bathing medium 1 (in mM): 10 $Ca(OH)_2$, 5 KOH, 2 $MgCl_2$, 13 dimethylglutaric acid, 5 HEPES pH 7.3, (*b*) after addition of 16 mM N-methylglucamine to the bathing medium 1, pH was adjusted with 10 mM dimethylglutaric acid and HEPES to 7.3 (bath 2). The pipette solution comprised (in mM): 50 KOH, 2 $MgCl_2$, 0.5 $CaCl_2$, 23 dimethylglutaric acid + HEPES pH 7.3. Data are low pass filtered at 300 Hz. C ≻ marks the zero current level. (*B*) Unitary current voltage characteristics. Pipette and bath solutions are as in *A*: bath 1 (●), bath 2 (○). Data are corrected for liquid junction potentials, which were 16 mV (bath 1) and 15 mV (bath 2).

amounts of Ca^{2+} (0.03 mM to 1 mM) added to the bath. The open state probability of the channel was derived from amplitude histograms (*see* Materials and Methods) and determined for a wide range of voltages and vacuolar

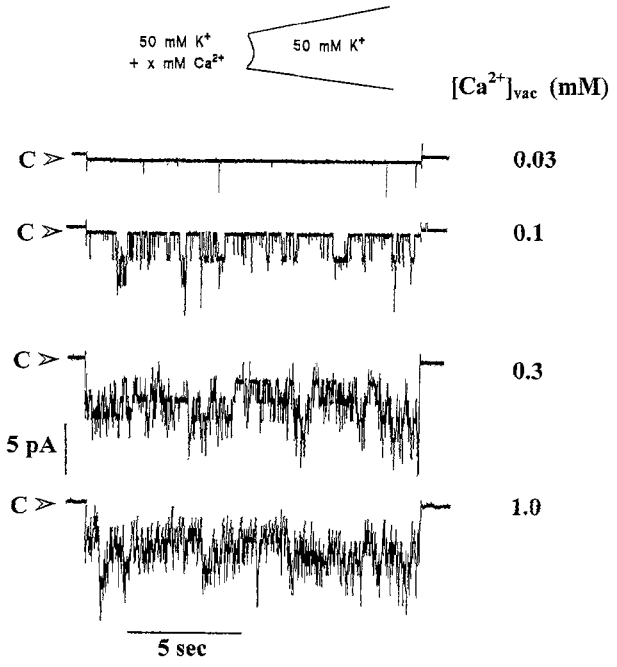

Fig. 5. Single channel traces from a vacuolar-side out patch. Pipette solution: Medium I; bath solution: Medium I plus $CaCl_2$ as indicated. The holding potential was stepped from 0 mV to −24 mV for 15 sec and then back to 0 mV. All conditions were tested on the same patch. Note the instantaneous activation of the channel. The data are low pass filtered at 500 Hz. C ≻ marks the zero current level.

Ca^{2+} concentrations (Fig. 6*A*.). For a given Ca^{2+} concentration, the open state probability P_o of the channel increases with negative-going voltage following a Boltzmann distribution:

$$P_o = \frac{P_o^{max}}{1 + e^{(V_{0.5} - V)\,(zF/RT)}}, \tag{4}$$

where P_o^{max} is the maximal open state probability, which here has a value of 0.053, $V_{0.5}$ is the membrane potential at which $P_o^{max}/2$ is reached, z is the gating charge and F, R, T have their usual meanings. Elevation of vacuolar Ca^{2+} shifts the voltage activation for channel gating to less negative voltages. Furthermore, $V_{0.5}$, which is an indication of voltage activation, changes by approximately 59 mV per decade change in lumenal Ca^{2+} ($[Ca^{2+}]_{vac}$) (Fig. 6*B*.). The gating charge z, however, does not show a clear dependence on vacuolar Ca^{2+} (Fig. 6*C*.) and the values are in accord with those obtained by us earlier with Ca^{2+} alone as a charge carrier ($z = -1.3$).

In order to determine the Ca^{2+} binding affinity to the gate and the number of Ca^{2+} ions which are needed to open the channel, the data from Fig. 6*A*. were plotted as a function of $[Ca^{2+}]_{vac}$ and fitted to the Hill equation (5):

$$P_o = \frac{P_o^{max}}{1 + \left(\frac{K_{0.5}}{V}\right)^n}, \tag{5}$$

where P_o^{max} is 0.053, $K_{0.5}$ is the Ca^{2+} concentration at which $P_o^{max}/2$ is reached and n is the Hill coefficient.

Figure 7*A* shows that the open state probability at $V = -41$ mV increases with a Hill coefficient of $n = 2$ when lumenal Ca^{2+} is elevated, which suggests that binding of two Ca^{2+} ions is needed to open the gate. Assuming that P_o^{max} does not significantly change over the voltage range considered (−7 mV to −41 mV) $n = 2$ gives the best fit to all data sets. The $K_{0.5}$ values for Ca^{2+} binding to the gate are shown in Fig. 7*B*. as a function of voltage in a semilogarithmic plot. The data points were fitted to the Woodhull model (Eq. 3) from which a $K_{0.5}^{V=0}$ of 1.39 ± 0.05 mM and a fractional electrical distance of $\delta = 0.58 \pm 0.03$ is derived. Since binding of two Ca^{2+} ions is involved in opening the gate, the individual Ca^{2+} ion only senses a fractional electrical distance of $\delta/2 = 0.29$ which indicates that the Ca^{2+} binding site for channel gating is located approximately 30% through the electric field of the membrane.

Effect of other Divalent Cations on Permeation and Channel Gating

The Table shows that other divalent cations such as Mg^{2+}, Sr^{2+}, Ba^{2+} can also permeate the channel with a permeability sequence of $Ca^{2+} \approx Sr^{2+} \approx Ba^{2+} > Mg^{2+} > K^+$ and a reverse sequence for the unitary conductance $K^+ > Mg^{2+} \approx Ba^{2+} > Sr^{2+} \approx Ca^{2+}$. With respect to gating, however, only Sr^{2+} can activate the channel to the same extent as Ca^{2+} (*data not shown*) while Mg^{2+} and Ba^{2+} are less effective than Sr^{2+} and K^+ does not have any effect at all (Fig. 8). Thus for gating the sequence is $Ca^{2+} \approx Sr^{2+} > Mg^{2+} \gg Ba^{2+}$. Mn^{2+} is also able to permeate the channel but the open frequency was low and activity was reduced to short openings. This is demonstrated in Fig. 8. which compares single channel current traces recorded at V = −68 mV with Sr^{2+}, Mg^{2+}, Ba^{2+} and Mn^{2+} as charge carriers (all tested at 10 mM).

Since Mg^{2+} is likely to occur naturally in the vacuole, its effect on ion permeation and channel activation was studied in more detail. Fig 9*A*. compares the effect of Mg^{2+} and Ca^{2+} (both tested at 1 mM and added to the lumenal side in a background of symmetrical 50 mM K^+) on the inward current. Mg^{2+} inhibits the inward current (mainly carried by K^+) to a lesser extent than Ca^{2+}, suggesting that Mg^{2+} has a lower affinity to the binding site. This is in accord with the lower permeability ratio ($P_{Mg^{2+}}$: $P_{K^+} \approx 9{:}1$) determined from reversal potential measurements.

With respect to channel gating, Mg^{2+} is much less effective than Ca^{2+} in activating the channel (*see also* Johannes et al., 1992*b*) and the activation voltage is shifted positive by roughly 100 mV (Fig. 9*B*.). Thus in the physiological voltage range the channel is rarely open when Ca^{2+} is replaced by Mg^{2+} which means that lumenal Ca^{2+} is still an effective modulator of channel gating when Mg^{2+} is present.

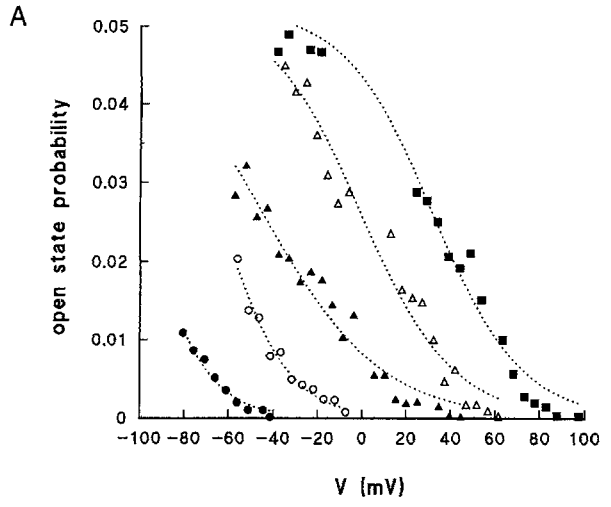

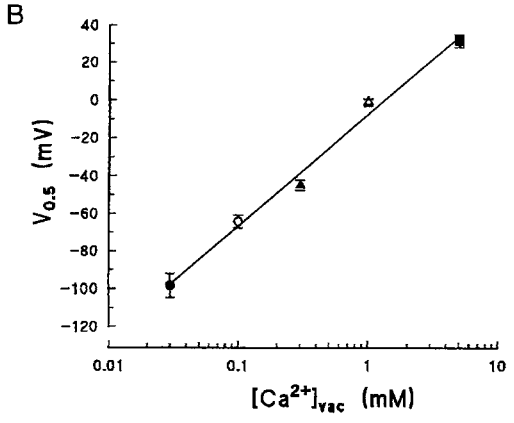

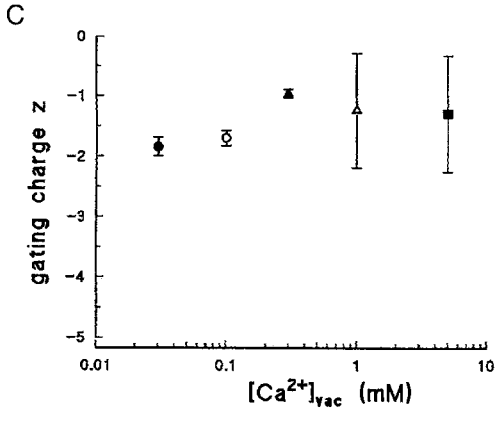

Fig. 6. (*A*) Voltage-dependence of the open state probability with (in mM): 0.03 $CaCl_2$ (●), 0.1 $CaCl_2$ (○), 0.3 $CaCl_2$ (▲), 1 $CaCl_2$ (△), and 5 $Ca(OH)_2$ (adjusted with dimethylglutaric acid to pH 7.3) (■) on the vacuolar side (bath) added to Medium I which was also used in the pipette. The solutions were successively tested in one lumenal-side-out patch. Similar results were observed in two other recordings. The dotted lines are nonlinear least squares fits of the data to the Boltzmann equation (4) with $P_o^{max} = 0.053$. The respective values for the gating charge z and for the membrane potential ($V_{0.5}$) at which $P_o^{max}/2$ is reached are depicted in the diagrams below (*B,C*). (*B*) Semi-logarithmic plot of $V_{0.5}$ as a function of the vacuolar Ca^{2+} concentration ($[Ca^{2+}]_{vac}$). The data are fitted by linear regression. $V_{0.5}$ is shifted to more positive potentials when lumenal Ca^{2+} is increased with a slope of 59.3 mV per log $[Ca^{2+}]_{vac}$. (*C*) Gating charge z as a function of vacuolar Ca^{2+} in a semi-logarithmic plot. The gating charge does not show a clear dependence of $[Ca^{2+}]_{vac}$.

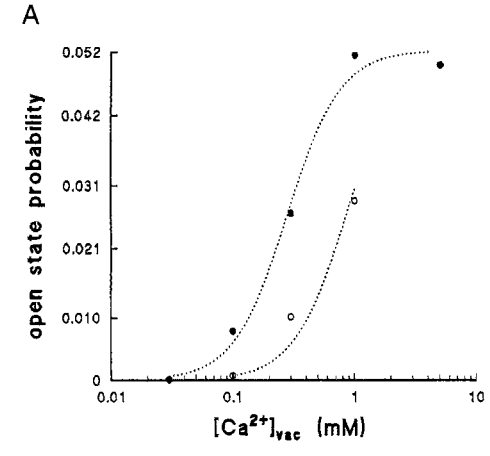

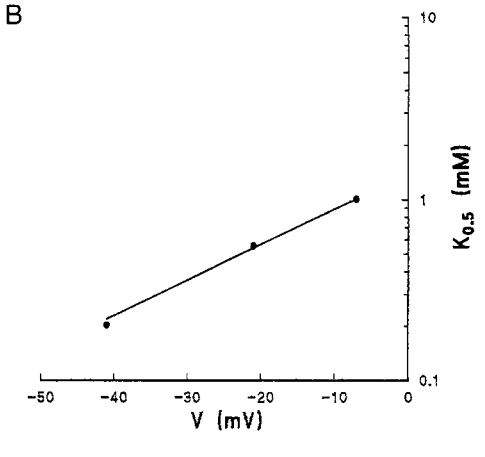

Fig. 7. (*A*) Ca^{2+}-dependence of the open state probability at a holding potential of −41 mV (●) and −7 mV (○). The data were taken from Fig. 6*A* and fitted by a nonlinear least-squares method to the Hill equation (Eq. 5). Best fits were obtained with $P_o^{max} = 0.053$ and a Hill coefficient of n = 2. The $K_{0.5}$ values for Ca^{2+} were 0.85 ± 0.10 mM at −7 mV and 0.28 ± 0.03 mM at −41 mV. (*B*) Voltage dependence of the $K_{0.5}$ values in a semi-logarithmic plot. The line represents the least-squares fit of the data to the Woodhull equation (Eq. 3) from which a fractional electrical distance of $\delta = 0.58 \pm 0.03$ and a $K_{0.5}^{V=0}$ of 1.39 ± 0.05 mM for the Ca^{2+} binding site(s) is derived.

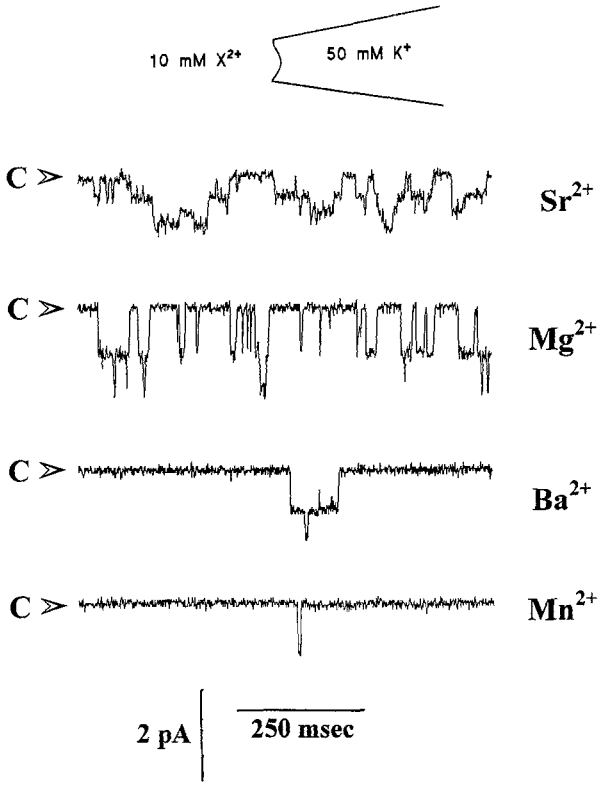

Fig. 8. Representative single channel current traces from lumenal-side-out patches with $SrCl_2$, $MgCl_2$, $BaCl_2$ and $MnCl_2$ (10 mM each) in the bath. Other conditions are as in Fig. 1. The holding potential was −68 mV. Data are low pass filtered at 500 Hz. C ≻ marks the zero current level.

Discussion

General Properties and Physiological Role

The Ca^{2+} release channel in the vacuolar membrane of sugar beet tap roots is activated by shifts in the vacuolar membrane potential over the negative (physiological) range. Channel gating is furthermore modulated by lumenal Ca^{2+} while Ca^{2+} on the cytoplasmic side leads to a strong inward rectification but has no significant effect on the Ca^{2+} inward current. With Ca^{2+}, Sr^{2+}, Mg^{2+} and Ba^{2+} as charge carriers, the single channel current saturates at negative vacuolar membrane potentials. Reversal potential measurements in bi-ionic conditions reveal a lower permeability with K^+ and Mg^{2+} than with Ba^{2+}, Sr^{2+} and Ca^{2+} while a reverse sequence is obtained for the unitary conductance which is highest with K^+. In comparison with other Ca^{2+} release channels in the vacuolar membrane of plant cells, the channel under investigation in this study bears many similarities with channels in guard cell vacuoles which open at negative membrane potentials (Allen & Sanders, 1994*a*; Johannes et al., 1994). Like the beet channel, the guard cell channel displays a higher channel activity when lumenal Ca^{2+} is elevated whereas cytoplasmic Ca^{2+} is ineffective in regulating Ca^{2+} release. In the guard cell channel, the unitary current also saturates at negative voltages and the sequence for permeabilities and unitary conductances obtained with mono- and divalent ions mirrors that observed in the beet channel. Both the beet and guard cell channels are inhibited by Gd^{3+}.

A different class of Ca^{2+} release channel in beet which is also activated over the physiological range of vacuolar membrane potentials has been described by

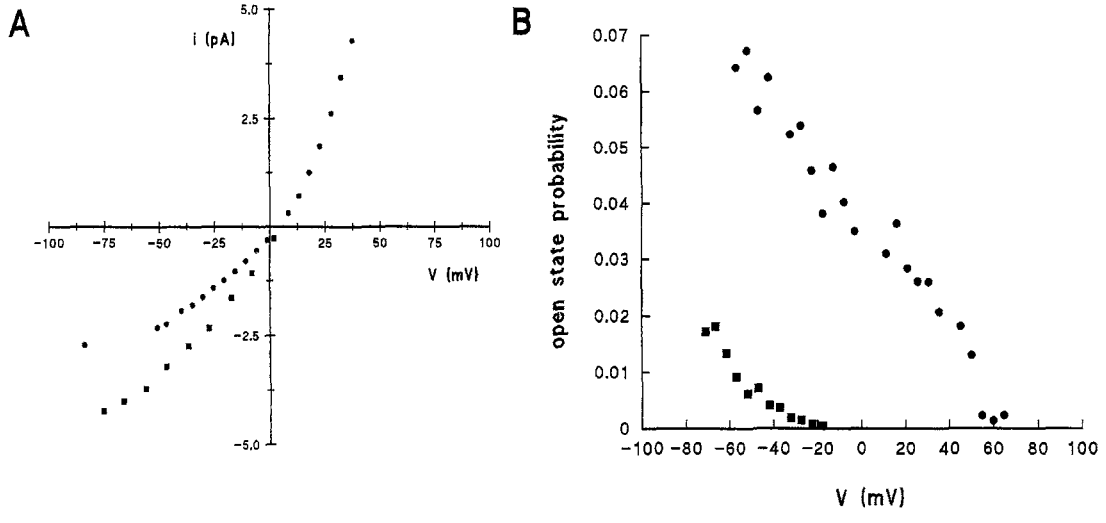

Fig. 9. Effect of 1 mM Ca^{2+} (●) and 1 mM Mg^{2+} (■) added successively to the bath of a single lumenal-side-out patch in symmetrical Medium I. (*A*) Unitary current voltage characteristics. Addition of Ca^{2+} causes a stronger reduction in the unitary inward current (mainly carried by K^+) than Mg^{2+}. (*B*) Voltage-dependence of the open state probability. Ca^{2+} is more effective in activating the channel than Mg^{2+}.

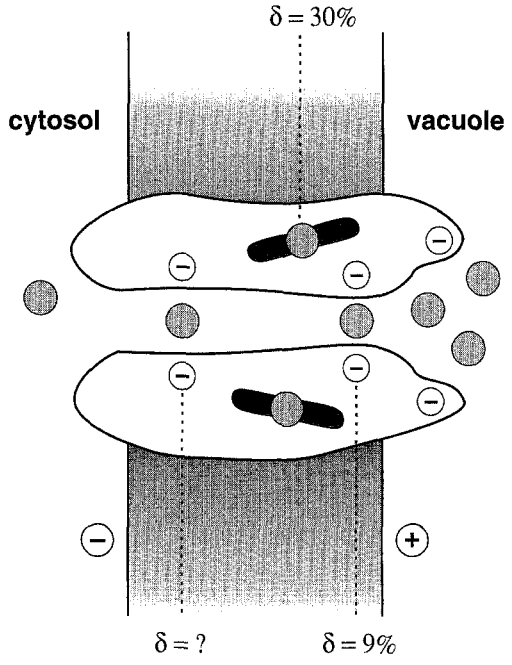

Fig. 10. Schematic diagram of Ca^{2+} binding sites in the voltage-gated Ca^{2+} release channel in the vacuolar membrane of a sugar beet. The two Ca^{2+} binding sites to the gate ($K_{0.5}^{V=0} = 1.39 \pm 0.05$ mM) are located 30% through the electric field of the membrane from the lumenal side (δ = 30%). A Ca^{2+} binding site in the pore lining region ($K_{0.5}^{V=0} = 0.292 \pm 0.003$ mM) which determines the Ca^{2+} selectivity has been found at δ = 9%. The location and affinity of the putative second binding site (δ = ?) has not been determined yet.

Gelli and Blumwald (1993). This channel shows a linear current voltage relationship with divalent cations and has a permeability sequence of $Ba^{2+} > Sr^{2+} > Ca^{2+}$ which is the same for the unitary conductance. Another feature which distinguishes the channel described by Gelli and Blumwald (1993) from that characterized in this study is its inhibition by micromolar cytoplasmic Ca^{2+} concentrations and its sensitivity to 1,4-dihydropyridines.

Ca^{2+}-permeable channels which open at putatively unphysiological positive membrane potentials can also function as Ca^{2+} release channels as recently proposed by Ward & Schroeder (1994). They discovered a Ca^{2+}-activated, highly K^+-selective channel in the vacuolar membrane of guard cells which, when activated, could depolarise the vacuolar membrane sufficiently to open the Ca^{2+}-permeable slowly activated channel (SV channel) which resides in the same membrane, leading to Ca^{2+}-activated Ca^{2+} release.

Thus in addition to ligand-gated Ca^{2+} release channels there are several distinct classes of voltage-operated channels in the vacuolar membrane which are able to mobilise Ca^{2+}. This is not surprising since it has been shown that the vacuole is a major site of Ca^{2+} release during stimulus-evoked elevation of cytoplasmic Ca^{2+} (Gilroy et al., 1991). Although it is so far difficult to link specific classes of Ca^{2+} release channels to a particular signal transduction pathway, the large variety of different Ca^{2+} release pathways could lead to a signal specific pattern of temporal and spatial Ca^{2+} changes in the cytoplasm which could define the specificity of the response.

Selectivity and Ion Permeation

In bi-ionic conditions, the voltage-gated Ca^{2+} channel in the vacuolar membrane of sugar beet tap roots exhibits an inverse relationship between the absolute permeability determined by the unitary current and the permeability ratio calculated from the reversal potential. Thus ion permeation through this channel is not independent but displays competition for binding site(s) in the channel pore. This has also been observed in L-type Ca^{2+} channels in animal cells where high affinity binding sites inside the channel pore have been mapped with respect to their binding affinity and location within the dielectric field of the membrane (Rosenberg & Chen, 1991). Using a similar strategy to that adopted in those studies, the location and Ca^{2+} affinity of the binding site in the beet channel was determined by evaluating the ability of Ca^{2+} ions to block the unitary K^+ current. From the concentration- and voltage-dependent block of the K^+ inward current by lumenal Ca^{2+} we detected a binding site with an affinity constant for Ca^{2+} of $K_{0.5}^{V=0} = 0.29$ mM which is located 9% through the electric field of the membrane from the lumenal side (Fig. 10.).

Compared with L-type Ca^{2+} channels which have Ca^{2+} binding constants in the micromolar range (Tsien et al., 1987), the vacuolar Ca^{2+} channel in *Beta vulgaris* exhibits only a moderate selectivity for Ca^{2+} over more abundant monovalent cations. This is also reflected in the permeability ratio $P_{Ca^{2+}}:P_{K^+}$ of 14–18:1 measured in bi-ionic conditions. This value, however, is in good agreement with those determined for other voltage-gated Ca^{2+} channels so far detected in plant cells.

Ca^{2+}-permeable channels in the vacuolar membrane of guard cells from *Vicia faba* (Allen & Sanders, 1994*a*) and *Commelina communis* (Johannes et al., 1994) have permeability ratios for Ca^{2+} over K^+ of 6:1 and 15:1, respectively. Studies on other vacuolar Ca^{2+}-permeable channels including those which open at unphysiological (positive) membrane potentials, yield permeability ratios between $P_{Ca^{2+}}:P_{K^+}$ = 20–23:1 in cell cultures of *Beta vulgaris* (Gelli & Glumwald, 1993) and $P_{Ca^{2+}}:P_{K^+}$ = 3:1 in slowly activated vacuolar channels in guard cells (Ward & Schroeder, 1994). However, a high Ca^{2+} selectivity as observed in animal channels is not needed for Ca^{2+} release channels in the vacuolar membrane of plant cells since the most permeant ions (e.g., K^+) are likely to be in equilibrium between the cytoplasm and vacuolar lumen whereas the Ca^{2+} gradient across the vacuolar membrane is steep. Thus opening of a Ca^{2+}-permeable channel would predominantly lead to Ca^{2+} influx into the

cytosol even when the relative permeability for Ca^{2+} is low (Ward & Schroeder, 1994). As argued by Bertl & Slayman (1992) a low permeability ratio for Ca^{2+} over K^+ also prevents the large depolarization of the vacuolar membrane which is expected when a highly Ca^{2+}-selective channel opens. In the case of the Ca^{2+} release channel which is inactivated at positive voltages as described in the present study, the relatively high K^+ permeability would thus enable a sustained Ca^{2+} release.

It should be noted, however, that all these selectivity determinations are based on the assumption of independent ion movement. Thus, our finding that the Ca^{2+} release channel in the vacuolar membrane of sugar beet exhibits characteristics of a multi-ion pore implies that the permeability ratios derived from the Goldman-Hodgkin-Katz equation are of qualitative nature and should therefore not be taken as absolute. A more accurate determination, however, would require complex equations based on a much more detailed knowledge of the interactions between ions and the channel protein than we have attempted in this study.

A detailed investigation regarding the mechanism of ion permeation has not been carried out for plant Ca^{2+} channels. However, some of the results obtained in other studies suggest that in many cases Ca^{2+} selectivity is achieved by its affinity to a binding site rather than rejection from a molecular sieve. The Ca^{2+}-permeable channel in the vacuolar membrane of guard cells of *Commelina communis* (Johannes et al., 1994) and *Vicia faba* (Allen & Sanders, 1994*a*) has a much larger unitary current with K^+ than with Ca^{2+} in spite of the higher relative permeability for Ca^{2+}. The vacuolar Ca^{2+} release channel reported by Gelli and Blumwald (1993) shows saturation of the unitary current (measured at V = –60 mV) when the concentration of divalent cations is increased: the respective $K_{0.5}$ values for Ba^{2+}, Sr^{2+}, and Ca^{2+} are 13.3, 18.1 and 24.3. However, bi-ionic instead of symmetrical solutions were used and the shifts in the reversal potential have not been accounted for.

High affinity binding sites for Ca^{2+} have been postulated for voltage-gated Ca^{2+}-permeable channels in the plasma membrane of wheat roots (Piñeros & Tester, 1995) which display a large unitary current under physiological conditions, and also for stretch-activated channels in the epidermis of onion bulbs (Ding & Pickard, 1993).

A more thorough investigation on Ca^{2+} binding sites has been carried out on the large conductance K^+ channel in the vacuolar membrane of *Chara* which like the beet channel in this study has a binding site close to the vacuolar lumen (Laver, 1992). However, it is not clear if the *Chara* channel is Ca^{2+}-permeable.

Evidence for a Multi-ion Pore

In L-type Ca^{2+} channels in animal cells at least two high affinity Ca^{2+} binding sites have been postulated and the concentration-dependent saturation of the unitary current (or conductance) in symmetrical solutions yielded $K_{0.5}$ values which were several orders of magnitude higher than those obtained from studies in which the block of univalent ionic current by Ca^{2+} was tested (Tsien et al., 1987). It was suggested that the occupancy of a first binding site decreases the binding affinity for a second ion by electrostatic repulsion. Simultaneously, binding of the second Ca^{2+} also increases the off-rate of the ion bound first, ensuring a high rate of Ca^{2+} translocation in spite of the high Ca^{2+} binding affinity. The Ca^{2+}-permeable channel in the vacuolar membrane of sugar beet also conducts Ca^{2+} at a higher rate (0.5 pA = $1.56 \cdot 10^6$ ions per second) than that which can be expected from simple dissociation of Ca^{2+} from its binding site. Even at a diffusion limited forward rate of 10^9 M^{-1} $second^{-1}$, for the observed affinity constant of 0.29 mM Ca^{2+} a 5-fold lower turnover rate of $3 \cdot 10^5$ ions per second would be expected. Therefore multiple binding sites in the channel pore with electrostatic interactions between ions are likely to exist.

Since the outward (K^+) current is completely blocked with 0.03 mM Ca^{2+} on the cytoplasmic side, our experimental system did not allow characterization of Ca^{2+} binding sites at the cytoplasmic face of the membrane. However, reversal potential measurements in mixtures of Ca^{2+} and K^+ at the vacuolar side showed permeability ratios about three-fold lower than in bi-ionic conditions (Fig. 3.) which is consistent with the notion of a multi-ion pore (Hille, 1992). Furthermore, attempts to simulate the measured current-voltage curves using an Eyring rate constant model with one energy well (defined by the binding constant) and two variable barriers (Lewis & Stevens, 1979) failed. In particular it was not possible to obtain the observed saturation of the single channel calcium current with voltage and the correct reversal potential with the same parameters. Thus more complex models with more than one binding site which allow for electrostatic interaction between ions in the pore (Hille & Schwarz, 1978) need to be considered. These, however, have far too many free parameters to be independently determined from our experiments.

Alternative models, originally developed for carrier-mediated transport, where Ca^{2+} binds externally and ion translocation involves conformational changes in the channel protein (e.g., Klieber & Gradmann, 1993) have not been considered in this study. These models imply that the conformational changes in the channel must be at least as fast as its turnover rate. At present there is no direct experimental evidence to support this view of channel function.

Other Parameters which Influence Ion Permeation

While the voltage- and dose-dependent block of K^+ current by vacuolar Ca^{2+} indicates an energy minimum

(Ca^{2+} binding site) inside the pore, the voltage-independent saturation of the unitary current suggests that the highest barrier the calcium ion has to overcome lies outside the electric field of the membrane. This limitation of the unitary current could be determined by an intrinsic property of the channel or by diffusion-limited entry of Ca^{2+} into the pore (Läuger, 1976). In the well characterized large conductance K^+ channel in the vacuolar membrane of *Charophyte* algae, the unitary K^+ current also exhibits strong saturation at extreme voltages which has been attributed to diffusion limitation (Laver, Fairley & Walker, 1989). Nevertheless, for the *Chara* K^+ channel the saturation current depends on the K^+ concentration and is influenced by the ionic composition of the transmembrane side (Laver et al., 1989), whereas the Ca^{2+}-permeable channel in beet has an absolute limitation in the unitary current of about 0.5 pA when Ca^{2+} is used as a charge carrier. This value is independent of vacuolar Ca^{2+} in the tested range of 5–40 mM and is unaffected by changes in cytoplasmic Ca^{2+} (Johannes et al., 1992*a*). We therefore believe that this saturation represents a limitation of the turnover rate within the channel itself, rather than diffusion-limited entry. In any case, the strong saturation of the unitary current with voltage also sets limits for the unitary conductance. Thus, a Ca^{2+} concentration-dependent saturation of the unitary conductance would in this case not necessarily be attributable to saturation of a Ca^{2+} binding site.

Negative surface charges at the mouth of the channel also have profound implications for ion permeation (Green & Andersen, 1991). Surface charges at the cytoplasmic side of the large conductance K^+ channel in *Chara* have been characterized by measuring the shift of voltage-dependent parameters in response to changes in the ionic strength of the cytoplasmic environment (Laver & Fairley-Grenot, 1994).

Evidence for negative surface charges at the vacuolar entrance of the Ca^{2+}-permeable channel in sugar beet arises from the ability of impermeant cations like N-methylglucamine to reduce the unitary Ca^{2+} current and to increase the open frequency of the channel (Fig. 4.). Other large cations such as tris[hydroxymethyl]aminomethane (Tris), choline and 1,3-bis[tris(hydroxymethyl)methylamino]-propane (BTP) evoke a similar response which is dependent on the concentration and molecular weight of the cations tested (Johannes & Sanders, *unpublished results*). Tris, however, which has been used as a pH buffer in some experiments (cf. Fig. 1.; Fig. 8.) has the weakest effect and only interferes with the measured parameters at concentrations >5 mM. Addition of large anions (gluconic acid, $HEPES^-$, dimethylglutaric acid) does not have any effect on the single channel current or gating even at high concentrations.

The results suggest that these large cations interact with negative charges at the mouth of the pore and obstruct the entrance of Ca^{2+}. However, more information is needed to describe these effects quantitatively.

Effects of Ca^{2+} on Channel Gating

In addition to its blocking effect on the unitary K^+ current, the presence of Ca^{2+} on the vacuolar side was necessary to activate the channel. We find that Ca^{2+} concentrations in the range 0.03 to 5 mM modulate channel activity over the physiological range of membrane potentials by shifting the threshold for voltage activation to less negative voltages (Fig. 6*A,B.*). Since addition of Mg^{2+} exerted a much weaker effect than equimolar concentrations of Ca^{2+} (Fig. 9*B.*) a simple screening of negative surface potentials at the channel mouth (*see above*) can be ruled out as a mechanism.

The voltage- and Ca^{2+}-dependent activation of the channel reveals Ca^{2+} binding sites on the gate ($K_{0.5}^{V=0}$ = 1.39 mM) which are located approximately 30% through the electric field of the membrane from the vacuolar side (Fig. 10.). Binding of two Ca^{2+} ions is needed to open the gate.

Apart from voltage-gated Ca^{2+} channels in the vacuolar membrane of guard cells whose open probability is also enhanced with increasing vacuolar Ca^{2+} (Allen & Sanders, 1994*a*), Ca^{2+} effects on gating of vacuolar channels have mostly been observed upon variation of cytoplasmic Ca^{2+}. In the vacuolar K^+ channel in *Chara,* channel opening involves binding of three Ca^{2+} with an affinity constant of 0.5–5 μM and the respective binding sites are located approximately 4% through the electric field of the membrane from the cytoplasmic side (Laver & Walker, 1991). Inward rectifying Ca^{2+}-permeable cation channels which are activated by micromolar cytoplasmic Ca^{2+} concentrations in the presence of reducing agents have been found in the vacuole of yeast cells (Bertl & Slayman, 1990; Bertl et al., 1992).

The SV channel which opens at unphysiological positive vacuolar membrane potentials is also activated by cytosolic Ca^{2+}, and respective studies revealed a Hill coefficient of 1 and a binding constant of 1.5 μM ($V = 80$ mV) (Hedrich & Neher, 1987). Ward and Schroeder (1994) recently reported that these channels are Ca^{2+}-permeable (permeability ratio Ca^{2+}:K^+ = 3:1).

In summary, vacuolar channels which are activated by cytosolic Ca^{2+} have a much higher affinity for Ca^{2+} binding ($K_{0.5}$ values in the micromolar range) than that observed in the calcium permeable beet channel which is activated by millimolar vacuolar Ca^{2+} ($K_{0.5}^{V=0}$ = 1.39 ± 0.05 mM). This reflects the different Ca^{2+} activities which reside in these two compartments (cytoplasm: 100 nM, vacuolar lumen: 1–10 mM; Felle, 1988). It is difficult to judge which physiological role the observed modulation of channel gating by vacuolar Ca^{2+} has and it remains to be determined whether local changes in Ca^{2+}

in the close vicinity of the channel entrance occur when Ca^{2+} is released from the vacuole.

We thank Ian Jennings for writing and implementing some of the software used in this study and Anna J. Bate for technical assistance. The work was supported by grants from the Biotechnology and Biological Sciences Research Council to E.J. (PDF/14) and DS (PG87/529).

References

Alexandre, J., Lassalles, J.P., Kado, R.T. 1990. Opening of Ca^{2+} channels in isolated red beet root vacuole membrane by inositol-1,4,5-trisphosphate. *Nature* **343:**567–570

Allen, G.J., Sanders, D. 1994*a*. Two voltage-gated, calcium release channels coreside in the vacuolar membrane of broad bean guard cells. *Plant Cell* **6:**685–694

Allen, G.J., Sanders, D. 1994*b*. Osmotic stress enhances the competence of *Beta vulgaris* vacuoles to respond to inositol 1,4,5-trisphosphate. *Plant J.* **6:**687–695

Barry, P.H., Lynch, J.W. 1991. Liquid junction potentials and small cell effects in patch-clamp analysis. *J. Membrane Biol.* **121:**101–117

Bertl, A., Blumwald, E., Coronado, R., Eisenberg, R., Findlay, G., Gradmann, D., Hille, B., Köhler, K., Kolb, H.A., MacRobbie, E., Meissner, G., Miller, C., Neher, E., Palade, P., Pantoja, O., Sanders, D., Schroeder, J., Slayman, C., Spanswick, R., Walker, A., Williams A. 1992. Electrical measurements on endomembranes. *Science* **258:**873–874

Bertl, A., Gradmann, D., Slayman, C.L. 1992. Calcium- and voltage-dependent ion channels in Saccharomyces cerevisiae. *Phil. Trans. R. Soc. London B* **338:**63–72

Bertl, A., Slayman, C.L. 1990. Cation-selective channels in the vacuolar membrane of Saccharomyces: Dependence on calcium, redox state, and voltage. *Proc. Natl. Acad. Sci. USA* **87:**7824–7828.

Brosnan, J.M., Sanders, D. 1990. Inositol trisphosphate-mediated Ca^{2+} release in beet microsomes is inhibited by heparin. *FEBS Lett.* **260:**70–72

Bush, D. 1993. Regulation of cytosolic calcium in plants. *Plant Physiol.* **103:**7–13

Cosgrove, D.J. & Hedrich, R. 1991. Stretch-activated chloride, potassium and calcium channels coexisting in plasma membranes of guard cells of *Vicia faba L. Planta* **186:**143–153

Ding, J.P., Pickard, B.G. 1993. Mechanosensory calcium-selective cation channels in epidermal cells. *Plant J.* **3:**83–110

Felle, H. 1988. Cytoplasmic free calcium in *Riccia fluitans L.* and *Zea mays:* Interaction of Ca^{2+} and pH? *Planta* **176:**248–255

Gelli, A., Blumwald, E. 1993. Calcium retrieval from vacuolar pools. Characterization of a vacuolar calcium channel. *Plant Physiol.* **102:**1139–1146

Gilroy, S., Fricker, M., Read, N.D., Trewavas, A.J. 1991. Role of calcium in signal transduction of *Commelina* guard cells. *Plant Cell* **3:**333–344

Green, W.N., Andersen, O.S. 1991. Surface charges and ion channel function. *Annu. Rev. Physiol.* **53:**341–359

Hamill, O.P., Marty, A., Neher, E., Sakmann, B., Sigworth, F.J. 1981. Improved patch clamp techniques for high-resolution current recording from cells and cell-free membrane patches. *Pfluegers Arch.* **391:**85–100

Hedrich, R., Neher, E. 1987. Cytoplasmic calcium regulates voltage-dependent ion channels in plant vacuoles. *Nature* **329:**833–836

Hille, B. 1992. Ionic channels of excitable membranes, 2nd edition. Sinauer Associates, Sunderland, MA

Hille, B., Schwarz, W. 1978. Potassium channels as multi-ion single-file pores. *J. Gen. Physiol.* **72:**409–442

Johannes, E., Allen G.J., Sanders, D. 1994. Voltage-gated Ca^{2+} release channels in the vacuolar membranes from beet storage roots and guard cells. *In:* Membrane Transport in Plants and Fungi: Molecular Mechanisms and Control. SEB Symposia Vol. 48. M.R. Blatt, R.A. Leigh, and D. Sanders, editors. pp. 113–122. The Company of Biologists, Ltd., Cambridge

Johannes, E., Brosnan, J.M., Sanders, D. 1991. Calcium channels and signal transduction in plant cells. *Bioessays* **13:**331–336

Johannes, E., Brosnan, J.M., Sanders, D. 1992*a*. Parallel pathways for intracellular Ca^{2+} release from the vacuole of higher plants. *Plant J* **2:**97–102

Johannes, E., Brosnan, J.M., Sanders, D. 1992*b*. Calcium channels in the vacuolar membrane of plants: multiple pathways for intracellular calcium mobilization. *Phil. Trans. R. Soc. London B* **338:**105–112

Klieber, H.-G., Gradmann, D. 1993. Enzyme kinetics of the prime K^+ channel in the tonoplast of *Chara:* selectivity and inhibition. *J. Membrane Biol.* **132:**253–265

Läuger, P. 1976. Diffusion-limited ion flow through pores. *Biochim. Biophys. Acta* **455:**493–509

Laver, D.R. 1992. Divalent cation block and competition between divalent and monovalent cations in the large-conductance K^+ channel from *Chara australis. J. Gen. Physiol.* **100:**269–300

Laver, D.R., Fairley, K.A., Walker, N.A. 1989. Ion permeation in a K^+ channel in *Chara australis:* direct evidence for diffusion limitation of ion flow in a maxi-K^+ channel. *J. Membrane Biol.* **108:**153–164

Laver, D.R., Fairley-Grenot, K.A. 1994. Surface potentials near the mouth of the large-conductance K^+ channel from *Chara australis:* A new method of testing for diffusion-limited ion flow. *J. Membrane Biol.* **139:**149–165

Laver, D.R., Walker, N.A. 1991. Activation by Ca^{2+} and block by divalent ions of the K^+ channel in the membrane of cytoplasmic drops from *Chara australis. J. Membrane Biol.* **120:**131–139

Leigh, R.A., Wyn-Jones, R.G. 1984. A hypothesis relating critical potassium concentrations for growth to the distribution and functions of this ion in the plant cell *New Phytol* **97,**1–13

Lewis, C.A., Stevens, C.F. 1979. Mechanism of ion permeation through channels in a postsynaptic membrane. *In:* Membrane Transport Processes, Vol. 3. C.F. Stevens, and R.W. Tsien, editors. pp. 133–151. Raven Press, New York

Maathuis, F.J.M., Sanders, D. 1993. Energization of potassium uptake in *Arabidopsis thaliana. Planta* **191:**302–307

Neher, E. 1992. Correction for liquid junction potentials in patch clamp experiments. *Methods Enzymol.* **207:**123–131

Pantoja, O., Gelli, A., Blumwald, E. 1992. Voltage-dependent calcium channels in plant vacuoles. *Science* **255:**1567–1570

Piñeros, M., Tester, M. 1995. Characterization of a voltage-dependent Ca^{2+}-selective channel from wheat roots. *Planta,* **195:**478–488

Ping, Z., Yabe, I., Muto, S. 1992*a*. Voltage-dependent Ca^{2+} channels in the plasma membrane and the vacuolar membrane of *Arabidopsis thaliana. Biochim. Biophys. Acta* **112:**287–290

Ping, Z., Yabe, I., Muto, S. 1992*b*. Identification of K^+, Cl^-, and Ca^{2+} channels in the vacuolar membrane of tobacco cell suspension cultures. *Protoplasma* **171:**7–18

Plant, P.J., Gelli, A., Blumwald, E. 1994. Vacuolar chloride regulation of an anion-selective tonoplast channel. *J. Membrane Biol.* **140:**1–12

Rea, P.A., Sanders, D. 1987. Tonoplast energization: Two H^+ pumps, one membrane. *Physiol. Plant.* **71:**131–141

Rosenberg, R.L., Chen, X.-H. 1991. Characterization and localization

of two ion-binding sites within the pore of cardiac L-type calcium channels. *J. Gen. Physiol.* **97:**1207–1225

Schroeder, J.I., Thuleau, P. 1991. Ca^{2+} channels in higher plant cells. *Plant Cell* **3:**555–559

Skoog, D.A., West, D.M. 1982. Fundamentals of analytical chemistry. Saunders College Publishing, Philadelphia

Tsien, R.W., Hess, P., McCleskey, E.W., Rosenberg, R.L. 1987. Calcium channels: Mechanisms of selectivity, permeation, and block. *Ann. Rev. Biophys. Biophys. Chem.* **16:**265–290

Thuleau, P., Ward, J.M., Ranjeva, R., Schroeder, J.I. 1994. Voltage-dependent calcium-permeable channels in the plasma membrane of a higher plant cell. *EMBO J.* **13:**2970–2975

Ward, J.M., Schroeder, J.I. 1994. Calcium-activated K^+ channels and calcium-induced calcium release by slow vacuolar ion channels in guard cell vacuoles implicated in the control of stomatal closure. *Plant Cell* **6:**669–683

Woodhull, A.M. 1973. Ionic blockage of sodium channels in nerve. *J. Gen. Physiol.* **61:**687–708

Yang, J., Ellinor, P.T., Sather, W.A., Zhang, J.F., Tsien, R.W. 1993. Molecular determinants of Ca^{2+} selectivity and ion permeation in L-type Ca^{2+} channels. *Nature* **366:**158–161